

1 **EFFECT OF FILLER NATURE AND CONTENT ON THE BITUMINOUS**
2 **MASTIC BEHAVIOUR UNDER CYCLIC LOADS**

3
4 Rodrigo Miró^a
5 r.miro@upc.edu

6
7 Adriana H. Martínez^{a,*}
8 adriana.martinez@upc.edu

9
10 Félix E. Pérez-Jiménez^a
11 edmundoperez@upc.edu

12
13 Ramón Botella^a
14 ramon.botella@upc.edu

15
16 Alex Álvarez^b
17 alexalvarez@yahoo.com

18
19 ^a Universitat Politècnica de Catalunya-BarcelonaTech, Jordi Girona 1–3, Mòdul B1,
20 08034 Barcelona, Spain

21
22 ^b University of Magdalena, Santa Marta, Carrera 32 # 22-08, Santa Marta, Magdalena,
23 Colombia

24
25 *Corresponding author
26 Tel.: +34 934017273
27 Fax: +34 934017064

28
29 **Abstract**

30
31 The role of the filler in asphalt mixtures is particularly important because of its
32 influence on mastic behaviour. The filler improves the resistance properties of bitumen
33 against the action of traffic loads and temperature. However, the filler can also
34 adversely affect bitumen in mastics excessively brittle and stiff due to inappropriate
35 design. For these reasons, it is interesting to investigate the effect of filler type and
36 content on mastic composition. This paper presents results from a strain sweep test
37 applied to bituminous mastics prepared with different filler types and contents at several
38 temperatures. The obtained stiffness modulus and failure strain results provide
39 information to assess the fatigue behaviour of the analysed mastics.

40
41 **Keywords:** Filler, Hydrated lime, Limestone, Granite, Volumetric concentration, Strain
42 sweep test

43
44 **1. Introduction**

45
46 Bituminous mastic obtained by mixing a filler with a bituminous binder greatly affects
47 the behaviour of the bituminous mixture. It is known that the addition of filler increases
48 the viscosity, stiffness and tensile strength of bitumen, leading to improved mixture
49 cohesion and reduced thermal susceptibility [1].

50

51 The most extensively studied physico-chemical variables of fillers related to mastic
52 behaviour are shape, size, nature and content [2-7]. Regarding the degree of packing of
53 filler particles, significant differences exist between natural fillers. Moreover, the degree
54 of packing has been found to affect both mastic and mixture behaviour, although no
55 correlation has been observed between test results of mastics and mixtures due to
56 complex interactions between the components of the mixture [8].

57
58 Some researchers have designed equipment to study the effect of filler particle size on
59 the viscoelastic properties of mastic. For example, Delaporte et al. [9, 10] developed an
60 annular shear rheometer and concluded that the use of ultrafine particles increases the
61 complex modulus of mastic at high temperature, compared to mastic prepared with
62 conventional fillers.

63
64 Clopotel et al proposed a novel method to estimate the change in viscosity of binders
65 due to the addition of fillers using glass transition temperature measurements [11].
66 Hesami et al. [12, 13] developed an empirical framework for determining mastic
67 viscosity as a function of filler concentration, demonstrating once again the complexity
68 of studying the behaviour of bituminous mastics.

69
70 It is equally important to highlight the adverse effects of high filler contents in mastic,
71 such as decrease in ductility, as too much filler can lead to fragile and brittle mastic.
72 Furthermore, the filler can sometimes have a hydrophilic character, i.e. a greater ability
73 to combine with water than with bituminous binder. This can result in a stripping
74 process of the mixture in the presence of water, resulting in loss of cohesion and
75 strength.

76
77 Therefore, the composition of the mastic should be carefully studied to select the
78 appropriate filler type and content to be incorporated in order to achieve the desired
79 physico-mechanical and volumetric properties. Former investigations by Rigden [14]
80 and Ruiz [15, 16] propose to limit filler addition to avoid an excessive volumetric
81 concentration in the filler-bitumen system; this "overfillerization" would lead to high
82 stiffness and the resulting loss of resistance to deformation, especially at low
83 temperatures.

84
85 Buttlar et al. [17] conducted an experimental program to predict the properties of mastic
86 in a wide range of temperatures and with different filler contents. They found that
87 particle-interaction reinforcement may play a minor role at low filler concentrations
88 whereas this mechanism is significant at high filler contents. They also concluded that
89 hydrated lime provided a much higher level of physicochemical reinforcement than
90 baghouse fillers.

91
92 A recent study on Test Methods and Specification Criteria for Mineral Filler Used in
93 HMA [18] conducted at the University of Wisconsin-Madison developed and set some
94 models to define indicators of workability, resistance to plastic deformation and
95 stiffness at low temperatures. Faheem et al. proposed a model for predicting the
96 complex modulus of the mastic as a function of the filler and bitumen properties [19].
97 Shen et al. [20] verified the application of the Ratio of Dissipated Energy Change
98 (RDEC) approach to evaluate the fatigue properties of viscoelastic materials,
99 (bituminous mixtures, mastics and binders), and found a unique relationship between
100 the parameter determined with this RDEC concept and the corresponding fatigue life,

101 independent of the material type and loading mode. Yin et al. [21] carried out a research
102 to assess the micromechanical models developed to predict complex modulus and
103 analyse the simplifications and limitations assumed in each model. They found that the
104 simplifications of some models affected the accuracy of the predictions,
105 underestimating some of the mastic properties or overestimating the experimental
106 results.

107

108 The present study aims to analyse the effect of filler type and content on the fatigue
109 behaviour of mastics at different temperatures by a strain sweep test (EBADE test, in
110 Spanish *Ensayo de BArrido de DEformaciones*, which stands for “strain sweep test”)
111 [22], developed at the Road Research Laboratory of the Universitat Politècnica de
112 Catalunya.

113

114 **2. Materials**

115

116 Three different mastics were prepared with 50/70 penetration grade bitumen and three
117 types of fillers: two natural types, a granite filler and a limestone filler, and a hydrated
118 lime filler. The mineralogical composition of the filler is the cause of the mechanical
119 bonding achieved by the filler-bitumen system, in addition to increasing the viscosity of
120 the bituminous mastic [23].

121

122 Mineral dust was added in volumetric concentrations. To this aim, the maximum
123 volume of filler which can be added to thicken the binder film was determined by a
124 sedimentation test to ensure that the binder film coats every filler particle. A viscous
125 hydrocarbon fluid with lower viscosity than bitumen, such as kerosene, can be used to
126 facilitate settlement.

127

128 The critical concentration determined by the sedimentation test corresponds to a
129 dispersion of filler particles in the bitumen moving as freely as possible but in contact
130 with each other, that is, when applied stresses in the viscous deformation of the
131 continuous filler-bitumen medium are such that frictional resistance between particles is
132 at a minimum.

133

134 Such a particle arrangement is expected in the sediment obtained by simple settling of
135 filler dispersion in a fluid medium chemically related to bitumens, like kerosene. Ruiz
136 [16] proposes a simple sedimentation test to find the critical value which guarantees
137 mastic viscous behaviour. This test is known as “Sediment concentration”, or most
138 commonly, “Critical concentration”, [24]. Bressi et al. used an equation to determine
139 critical filler concentration based on Rigden voids and methylene blue value [25].

140

141 In this study, critical concentration is calculated with the following equation:

142

$$C_s = \frac{V_{filler}}{V_s} = \frac{P_f/\gamma_f}{V_s} \quad (1)$$

143

144 where

145 C_s : critical concentration of filler

146 V_{filler} : volume of filler (cm³)

147 P_f : mass of filler (g)

148 V_s : settled volume of filler in anhydrous kerosene after 24 hours (cm³)

149 γ_f : density of filler (g/cm^3)

150

151 When filler is added to mixtures, bituminous mastic viscosity increases gradually with
152 increasing the volumetric concentration (C_v). In the case of asphalt bitumens, when C_v
153 $> C_s$, the biphasic system stops being viscous and an internal structure determining a net
154 non-Newtonian flow appears, which renders the mix stiff.

155

156 Different volumetric concentrations divided by the critical concentration (C_v/C_s) were
157 used for each filler, with C_v being determined by the following equation:

158

(2)

$$C_v = \frac{V_{\text{filler}}}{V_{\text{filler}} + V_{\text{bitumen}}} = \frac{P_f/\gamma_f}{P_f/\gamma_f + P_b/\gamma_b}$$

159

160 where

161 C_v : volumetric concentration of filler

162 V_{filler} and V_{bitumen} : volume of filler and volume of bitumen (cm^3), respectively

163 P_f and P_b : mass of filler and mass of bitumen (g), respectively

164 γ_f and γ_b : density of filler and of bitumen (g/cm^3), respectively

165

166 The C_v/C_s concentrations used in this study are 0 (neat bitumen), 0.5, 1.0 and 1.25.

167 Table 1 shows the characteristics of the bitumens and table 2 shows the density of the

168 fillers, as well as the critical concentration, and the volumetric and mass concentrations.

169

170

171 **Table 1.** Characteristics of bitumens (Source: REPSOL)

172

Characteristics	Unit	Standard	B50/70
Original Bitumen			
Penetration at 25°C	(0.1 mm)	EN 1426	59
Softening Point R&B	(°C)	EN 1427	50.2
Fraass Brittle Point	(°C)	EN 12593	-11
After RTFOT			
Mass Loss	(%)	EN 12607-1	0.02
Retained Penetration at 25°C	(%)	EN 1426	62
Increase in Softening Point	(°C)	EN 1427	7.0

173

174

175 **Table 2.** Characteristics of fillers

176

Filler Type	Density	Cs	Cv/Cs Ratio	f/b Ratio
Granite	2.662	0.330	0.5	0.51
			1	1.27
			1.25	1.82
Limestone	2.683	0.277	0.5	0.42
			1	1
			1.25	1.38
Lime	2.375	0.121	0.5	0.15
			1	0.32
			1.25	0.41

177

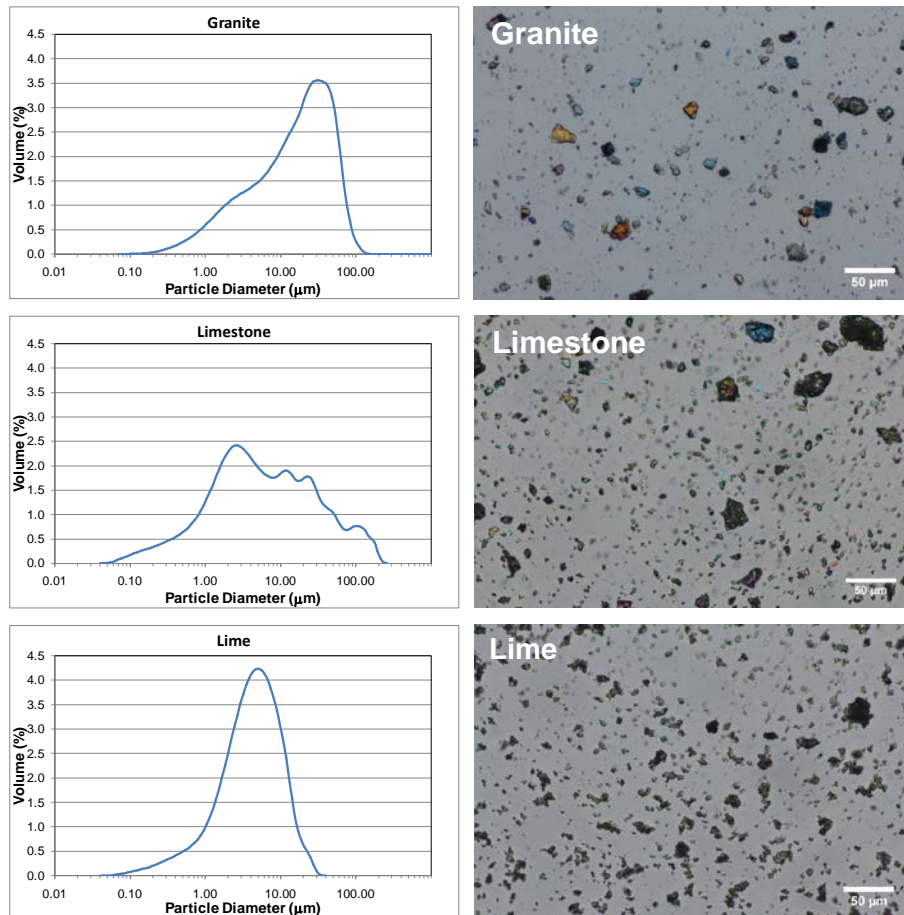


Figure 1. Filler particle shape and distribution

Particle size and shape affect the mechanical properties of mastics, such as stiffness, toughness, fracture energy, as stated by Antunes et al. and Movilla-Quesada et al. [26-29]. Figure 1 shows the particle size distribution of each filler, obtained with a *Laser Diffraction Particle Size Analyser*, together with an image of the particle shape and distribution, obtained with an optical microscope. The photographs indicate that the shapes of the largest granite particles are clearly different from those of the other fillers. It can also be seen that the limestone particle size is quite large (some of the particles are larger than 63 μm) and lime particles tend to lump despite the fact that the lime filler is the most homogeneous in terms of particle size distribution.

3. Testing method

All the specimens of mastic were fabricated with the aforementioned bitumen and fillers, mixing both materials uniformly before proceeding to the specimen moulding. The mastic specimens were cylinders of 20 mm of diameter and around 40 mm in height, Figure 2a. The type of the specimen is similar to that used by Molenaar et al. although the dimensions are greater [30]. The asphalt binder was heated to 145-155°C in the oven, except when granite filler was used at the higher volumetric concentration, for which it was necessary to increase the temperature by 30°C due to its high viscosity. Mastic mixtures were poured into the cylindrical moulds at 135-145°C, and after that the moulds were vibrated for 30 seconds. Specimens were left to cool at room temperature; after removing the specimens from the mould they were glued to a servo-hydraulic press in order to perform the tests, Figure 2b.

205



206
207

208 **Figure 2.** (a) Preparation of mastic specimens and (b) EBADE test set up

209

210 EBADE test is a cyclic tension-compression test at controlled strain. Several strain
211 amplitudes in ascending order in stages of 5,000 loading cycles at a frequency of 10 Hz
212 are applied.

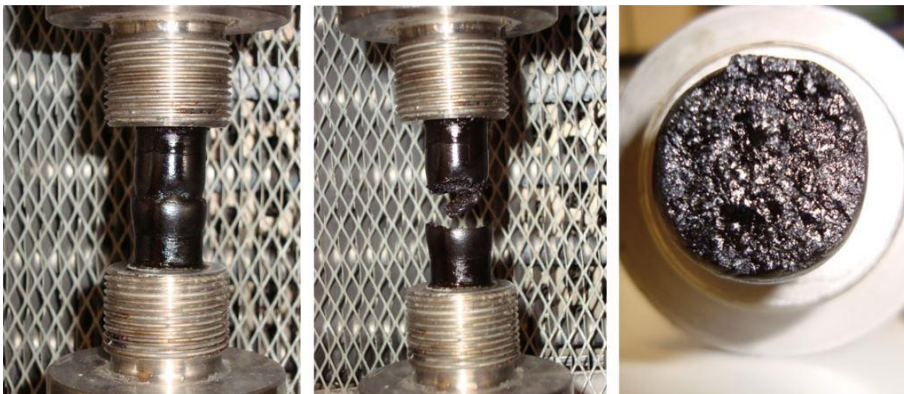
213

214 The strain amplitude applied in the first step is $7.6E-4$, and every 5,000 cycles the strain
215 increases in $7.6E-4$. This way the number of cycles and the strain amplitude are directly
216 related. The test finishes when the total failure of the specimen takes place.

217

218 Images taken during the performance of the test until failure of the specimen are
219 presented in Figure 3 as well as the appearance of the sample after having been tested.

220



221
222

223 **Figure 3.** EBADE test in mastics: (a) initial strain, (b) specimen failure, (c) specimen
224 appearance after failure

225

226 Several parameters can be computed during the test. The most important are maximum
227 stress, complex modulus and dissipated energy density, during each cycle. Stress can be
228 determined from equation (3):

229

$$230 \sigma = \frac{F}{S} \quad (3)$$

231

232 where σ (MPa) is the stress, F (N) is the applied load and S (mm^2) is the specimen cross
233 section.

234

235 Using the maximum stress and strain it is possible to obtain the complex modulus by
236 means of equation (4):

237

$$|E^*| = \frac{\sigma_{max}}{\epsilon_{max}} \quad (4)$$

238

239 where $|E^*|$ (MPa) is the complex modulus, σ_{max} (MPa) is the maximum stress

240 amplitude registered in a cycle and ϵ_{max} is strain amplitude imposed.

241

242 The initial modulus given by the test is obtained as the average of the moduli registered

243 in all cycles corresponding to the first strain step (amplitude of 7.6 E-4). At these low

244 strain levels the behaviour of the material is linear.

245

246 Due to the delay between stress and strain an ellipse is formed in the stress vs. strain plot.

247 The dissipated energy density is proportional to the area of the ellipse in the tension-

248 compression graph. To compute this area from the test data, the Gauss Determinant

249 Formula was used in the following equation:

250

$$DED = \frac{1}{2} [(\sigma_1\epsilon_2 + \sigma_2\epsilon_3 + \dots + \sigma_{n-1}\epsilon_n + \sigma_n\epsilon_1) - (\sigma_2\epsilon_1 + \sigma_3\epsilon_2 + \dots + \sigma_n\epsilon_{n-1} + \sigma_1\epsilon_n)] 10^6 \quad (5)$$

251

252 where DED (J/m^3) is Dissipated Energy Density and σ_i (MPa) and ϵ_i are the n values of

253 stress and strain obtained during a cycle.

254

255 Given the characteristics of the test, it is possible to obtain the strain at which the material

256 is completely broken, failure strain. Specifically, the typical shape of the curves of

257 dissipated energy density versus number of cycles allows easily determining the value of

258 the failure strain. The reason is that DED increases throughout the test with the number

259 of cycles to a maximum, after which it starts to decrease rather quickly as a result of the

260 specimen failure. Consequently, a new parameter called failure strain is defined as the

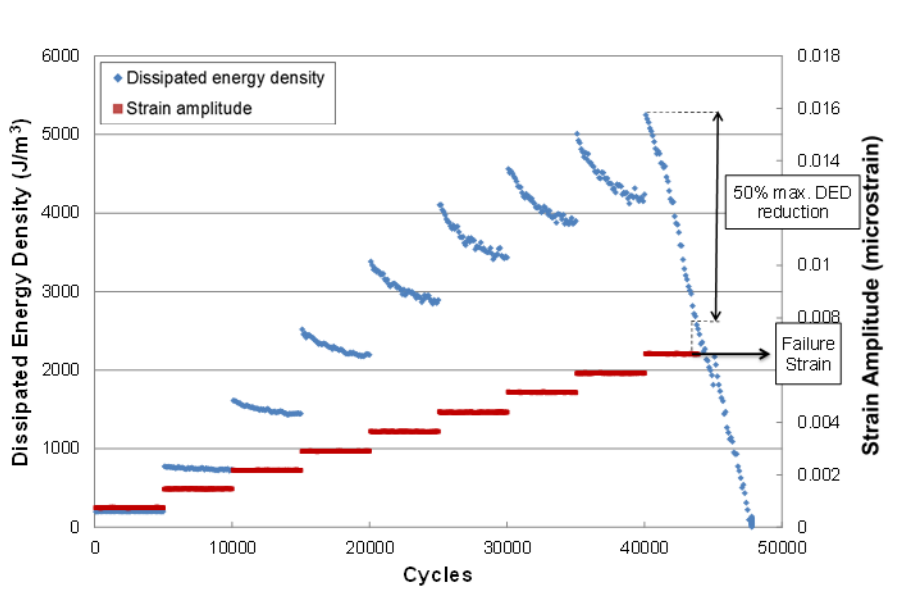
261 strain at which the dissipated energy density is reduced by 50% of the maximum value

262 reached during the test, Figure 4.

263

264

265



266

267 **Figure 4.** Failure criterion. Obtainment of failure strain

268

269 In this case, the test was performed at three different temperatures, 20, 10 and 0°C, in

270 order to evaluate the behaviour of different mastics under different conditions. At low

271 temperatures, mastics can show a more fragile response than at room temperature and
272 therefore, be more critical for the fatigue resistance. It is interesting to note that EBADE
273 test was used previously to analyze the fatigue response of different types of bitumen
274 (penetration, polymer modified and crumb rubber modified bitumens) at different
275 temperatures and the results obtained confirmed their agreement with those from DSR,
276 [31].

277

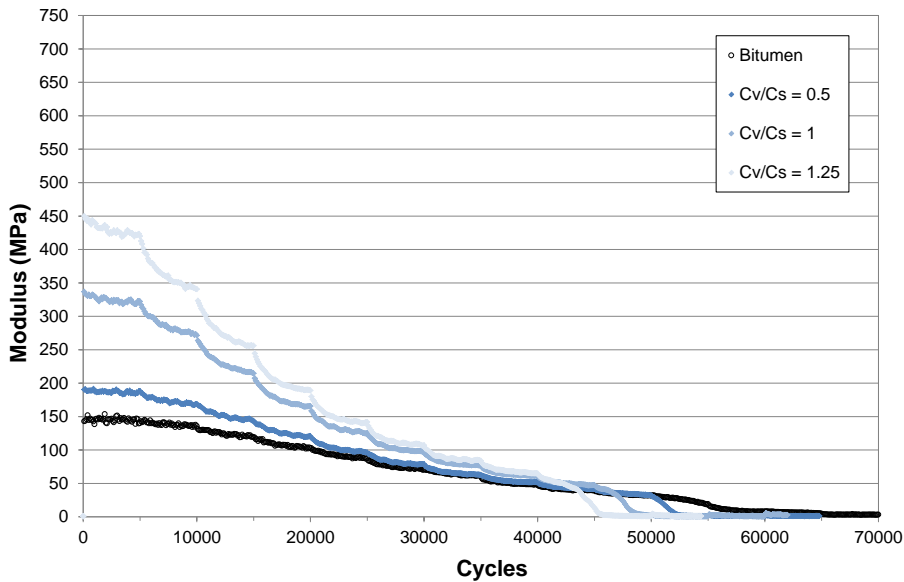
278 4. Analysis of results

279

280 As an example, figures 5 and 6 show the variation in stiffness modulus and dissipated
281 energy density with the number of cycles at 10°C for mastics obtained with the
282 limestone filler at different volumetric concentrations. It is clearly observed how
283 modulus at the first cycle and dissipated energy density increase with the increase in
284 volumetric concentration whereas the failure cycle gradually decreases.
285

285

286



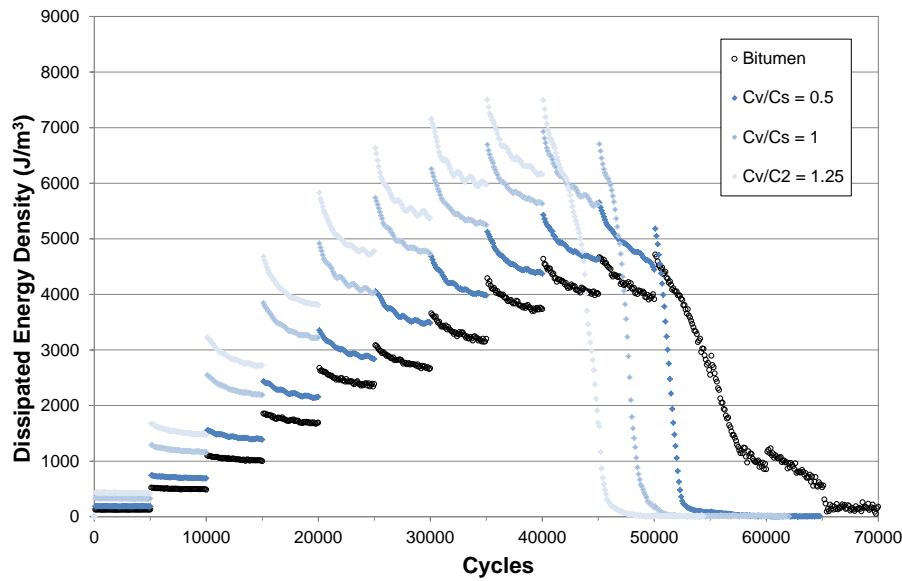
287

288

289

290

Figure 5. Stiffness modulus versus number of cycles at 10°C. Limestone filler



291
292
293
294
295
296
297
298

Figure 6. Dissipated energy density versus number of cycles at 10°C. Limestone filler

Table 3 summarizes the mean values of the parameters obtained from EBADE test at the three test temperatures for each mastic analysed.

Table 3. Results of EBADE test

Filler	Cv/Cs	f/b	Initial Modulus (MPa)			Failure Strain (μdef)		
			20°C	10°C	0°C	20°C	10°C	0°C
			Without Filler	-	-	29	148	350
Granite	0.5	0.51	61	234	569	9114	7784	6076
	1	1.27	116	423	1045	8734	6076	3038
	1.25*	1.82	174	565	1607	8354	4937	1898
Limestone	0.5	0.42	55	187	541	9492	8355	6582
	1	1	83	325	871	9114	7595	5696
	1.25	1.38	123	430	1103	8861	6835	4937
Lime	0.5	0.15	36	146	446	9492	8354	6835
	1	0.32	59	216	553	8734	7595	6076
	1.25	0.41	68	274	622	8734	6835	5316

299 (*): At this granite concentration, the mastic is excessively viscous; therefore, it was prepared at
300 a higher temperature than that used with the other fillers.

301

302 The variation in the stiffness modulus and failure strain with the volumetric
303 concentration used with each filler for the three test temperatures is plotted in figures 7
304 and 8.

305

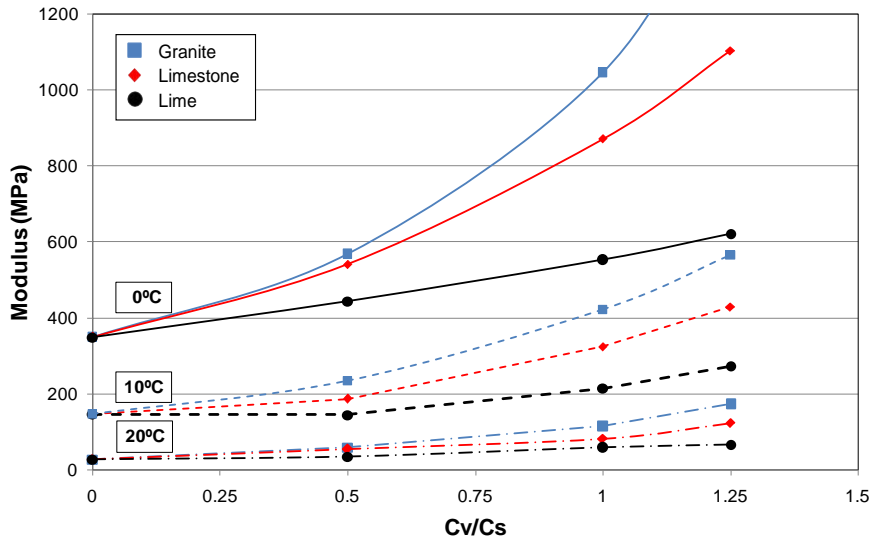
306 Figure 7 shows how the stiffness modulus of all mastics increases with decreasing the
307 temperature and increasing the filler concentration. Granite has the highest stiffness
308 increase with filler concentration, followed by limestone, whereas lime exhibits the
309 lowest value.

310

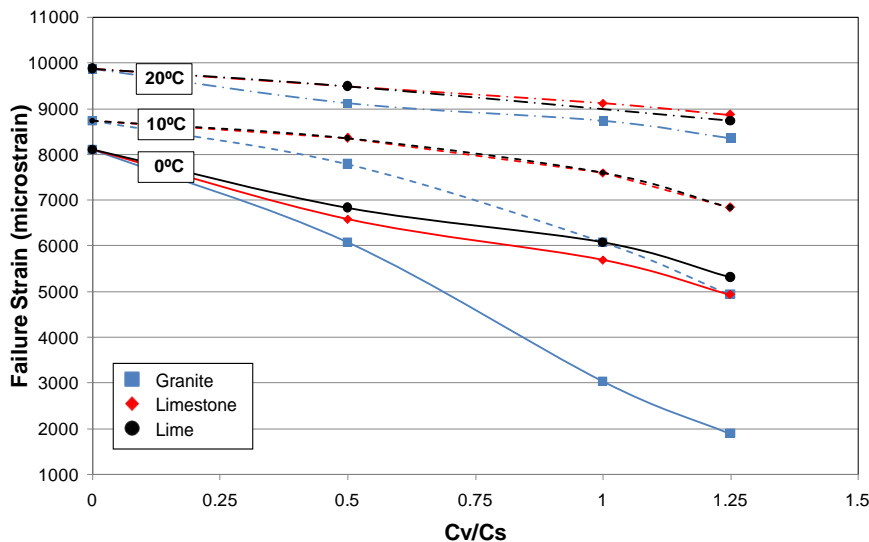
311

312

313 Consequently, the failure strain decreases with decreasing the temperature and increasing
 314 the filler concentration, Figure 8. At 20°C the behaviour of the three fillers is very
 315 similar. However, at 10°C and 0°C granite exhibits the greatest loss of ductility,
 316 especially at Cv/Cs higher than 0.5.
 317



318
 319 **Figure 7.** Stiffness modulus versus temperature and volumetric concentration for mastics
 320 manufactured with the three fillers
 321



322
 323 **Figure 8.** Failure strain versus temperature and volumetric concentration for mastics
 324 manufactured with the three fillers
 325

326 In general, if the volumetric concentration does not exceed the critical concentration, the
 327 addition of appropriate filler causes a moderate decrease in failure strain, but also a
 328 significant increase in the stiffness modulus. This improves the fatigue response of the
 329 mixture.

330
 331 As was shown in Figure 1, maximum particle size of lime is lower than those of
 332 limestone and granite. The effect of this variable on the mastic behaviour could have

333 prevented the modulus from increasing, as Ward and McDougal [32] and Kandhal and
334 Parker found [33]. As they stated, not all the fine materials act as a filler; they could act
335 as an extender of bitumen; although this hypothesis should be analysed in greater detail
336 in order to confirm this phenomenon.

337 If the variation of these parameters, i.e. stiffness modulus and failure strain, is
338 represented based on the filler/bitumen ratio by mass, Figures 9 and 10, some
339 differential aspects can be observed. The modulus increases with the mass of filler; the
340 variation for granite and limestone is very similar, in such a way that for the same f/b
341 ratio, the stiffness modulus is almost the same for both fillers. In contrast, a rapid
342 stiffening (modulus increase) of the mastic prepared with lime is observed with
343 relatively small amounts of this filler, as Figure 9 shows.

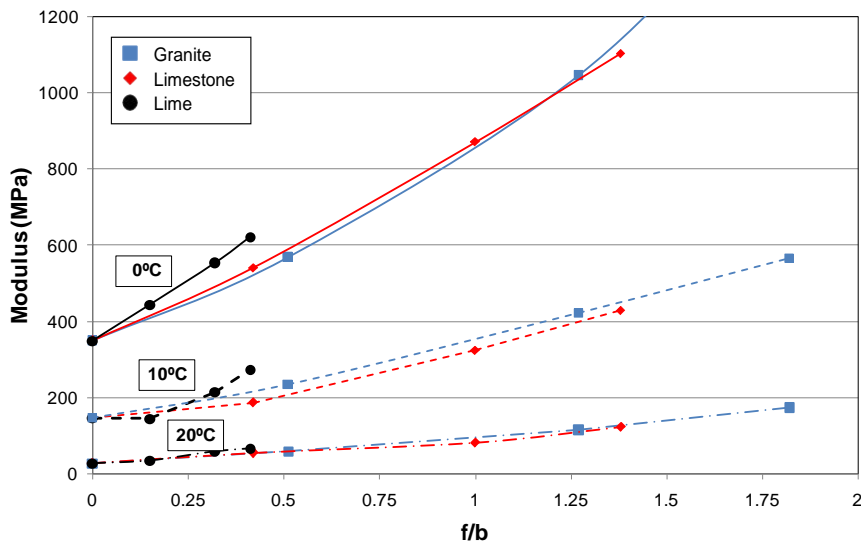
344

345 Moreover, the analysis of variation in failure strain with the filler/bitumen ratio by mass
346 shows again the difference in behaviour between lime and the other two fillers since the
347 failure strain decreases rapidly with increasing the mass of lime, Figure 10.
348 Additionally, although the stiffness modulus of the limestone and granite fillers is very
349 similar, now it is observed that the failure strain of granite is much lower than that of
350 limestone.

351

352 Extrapolation of the lime curves shows that it would be almost impossible to
353 manufacture mastics with the filler/bitumen ratios by mass specified in Spain (between
354 0.9 and 1.2 for AC mixtures), and that even at lower ratios the mastic would be very
355 stiff and undergo a brittle fracture, leading to a totally inappropriate behaviour.

356



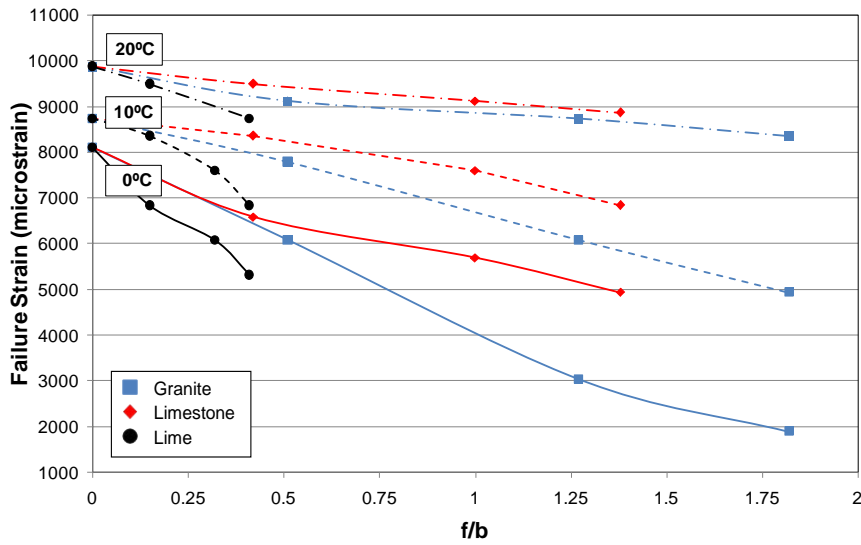
357

358

359

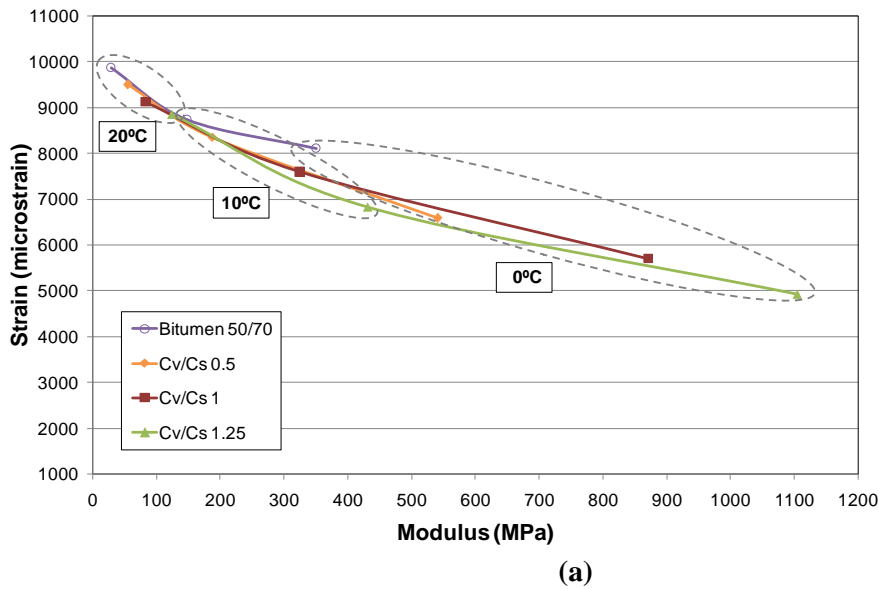
360

Figure 9. Stiffness modulus versus temperature and filler/bitumen ratio by mass for mastics manufactured with the three fillers



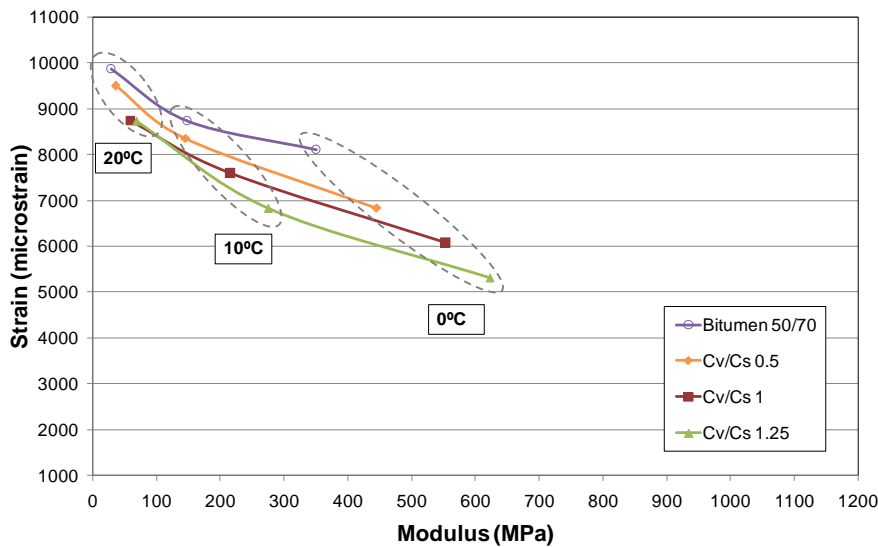
361
 362 **Figure 10.** Failure strain versus temperature and filler/bitumen ratio by mass for mastics
 363 manufactured with the three fillers
 364

365
 366 Finally, Figures 11a, 11b and 11c show the relationship between stiffness modulus and
 367 failure strain and the neat bitumen curve for each concentration of filler at all test
 368 temperatures. Comparison of these figures reveals clear differences in the behaviour of
 369 the mastics.
 370

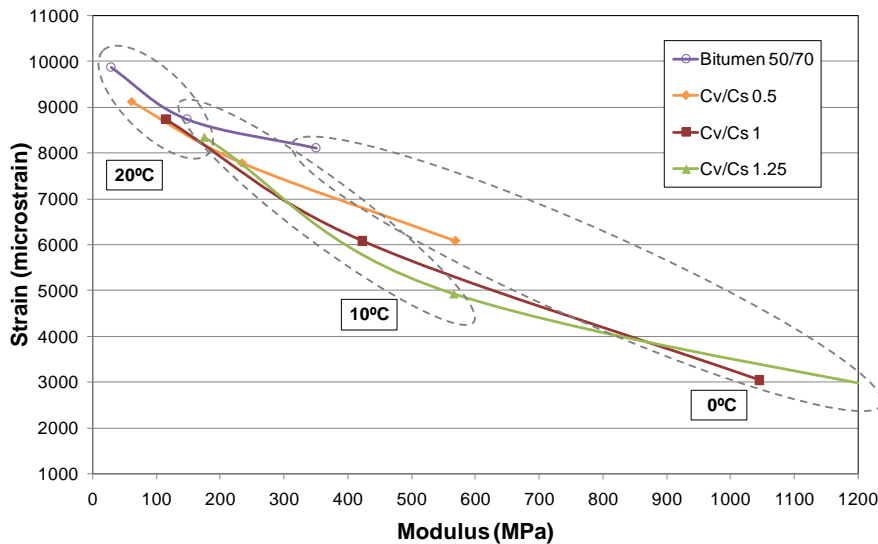


371
 372

(a)



(b)



(c)

373
374

375
376
377

Figure 11. Failure strain versus modulus at 20°C, 10°C and 0°C and different volumetric concentrations for the mastics manufactured with: (a) limestone, (b) lime and (c) granite

379

380

381

382

383

384

385

386

387

388

389

390

391

392

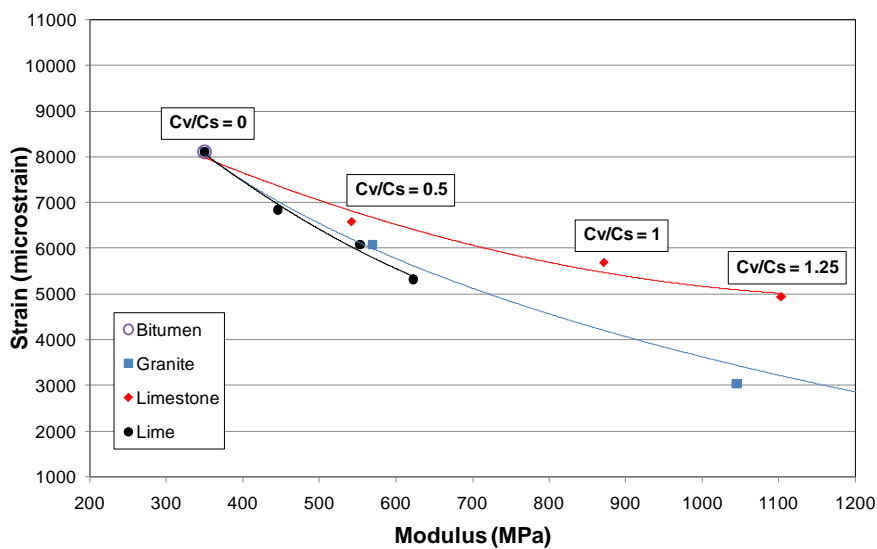
For the limestone filler, Figure 11a, the curves obtained at different temperatures and concentrations tend to overlap. The stiffness variation produced when increasing the filler content in the mastic shows a similar slope as that produced by the temperature decrease, although this does not mean that the variations are equivalent.

In the case of the lime filler, Figure 11b, the curves for each concentration tend to separate, remaining more or less parallel to each other. If points of equal temperature (surrounded by dashed ellipses) are joined, the slope of the resulting curves would be very different from the slope of the curves of equal filler content (equal Cv/Cs). So, the variation of failure strain and modulus is very different considering the temperature effect than considering the filler content effect. And in the case of granite, Figure 11c,

393 minor changes in behaviour are observed with increasing concentration at 20°C,
 394 whereas at low temperatures (0°C) the filler behaves significantly differently, showing a
 395 sharp increase in stiffness and fragility with increasing filler content.

396

397 Figure 12 shows the curves corresponding to the concentrations of the three fillers at the
 398 same test temperature, i.e. 0°C. All the curves tend to converge at the point representing
 399 the neat bitumen with decreasing volumetric concentration of filler in the mastic.
 400 Furthermore, the decrease in failure strain with increasing stiffness modulus is more
 401 pronounced for the lime and granite fillers. The latter performs worse since, at a given
 402 concentration of filler, the decrease in strain and increase in modulus are much more
 403 significant. The limestone filler has the best performance since the slope of the
 404 modulus-strain curve is smaller; that is, for the same increase in modulus the failure
 405 strain remains high.



406

407 **Figure 12.** Failure strain versus modulus at different volumetric concentrations at 0°C for the
 408 bitumen and the mastics manufactured with the three fillers.

409

410 4. Conclusions

411

412 This study investigates the effect of filler type and content on the fatigue behaviour of
 413 mastic at different temperatures (20, 10 and 0°C) by EBADE test. Three different
 414 mastics prepared with conventional 50/70 penetration grade bitumen and three types of
 415 fillers (two natural types, a granite and a limestone filler, and a hydrated lime) were
 416 analysed at different volumetric concentrations.

417

418 The following conclusions can be drawn from the obtained results:

419

420 - An increase in the volumetric concentration of filler in the mastic results in increased
 421 stiffness modulus and decreased failure strain, especially at lower temperatures, with the
 422 granite filler showing the highest variations. Granite has an average particle size and a
 423 clearly different particle shape.

424

425 - For the same volume ratios C_v/C_s , the limestone and lime fillers have similar ductility
 426 at all test temperatures. However, considering their mass proportions, a smaller amount

427 of lime than limestone or granite must be used as the increase in stiffness modulus and
428 decrease in strain occur at a much lower filler/bitumen ratio by mass.

429

430 - The modulus-strain curve of the limestone filler has the smallest slope, meaning that
431 this filler has the best fatigue behaviour. That is, the failure strain of limestone remains
432 high for the same increase in stiffness. Granite stiffens the mastic excessively, and a
433 content increase results in a significantly lower failure strain, especially at low
434 temperatures; reason why it could be recommendable to limit the amount of granite to
435 be used in the mixture. On the other hand, lime has the lowest stiffness modulus despite
436 exhibiting a high failure strain.

437

438

439 **Acknowledgements**

440

441 The authors would like to thank the Ministerio de Economía y Competitividad for its
442 assistance in the project PROFIS (BIA2012- 36508), established within the framework
443 of the VI Plan Nacional de Investigación Científica, Desarrollo e Innovación
444 Tecnológica. The authors would also like to acknowledge the company REPSOL for
445 supplying and characterizing the bitumen used in this study, and UPC researchers
446 Marilda Barra and Diego Aponte for their help in conducting the optical microscopy
447 tests.

448

449 **References**

450

451 [1] Tunnicliff, D.G. (1961). A Review of Mineral Filler. *Journal of the Association of*
452 *Asphalt Paving Technologists*, Vol. 31, pp.119-147.

453

454 [2] Harris, B.M. & Stuart, K.D. (1995). Analysis of Mineral Fillers and Mastics Used
455 in Stone Matrix Asphalt. *Journal of the Association of Asphalt Paving*
456 *Technologists*, Vol. 64, pp.54-95.

457

458 [3] Heukelom, W. & Wijga, P.W.O. (1971). Viscosity of Dispersions as Governed by
459 Concentration and Rate of Shear. *Journal of the Association of Asphalt Paving*
460 *Technologists*, Vol. 40, pp. 418-437.

461

462 [4] Tayebali, A.A., Malpass, G.A. & Khosla, N.P.. (1998). Effect of Mineral Filler
463 Type and Amount on Design and Performance of Asphalt Concrete Mixtures.
464 *Journal of the Transportation Research Record*, No. 1609, Transportation
465 Research Board of the National Academies, Washington, D.C., pp. 36-43.

466

467 [5] Wang, H., Al-Qadi, I.L.; Faheem, A.F., Bahia, H.U., Yang, S. & Reinke, G.H.
468 (2011). Effect of Mineral Filler Characteristics on Asphalt Mastic and Mixture
469 Rutting Potential. *Journal of the Transportation Research Record*, No. 2208,
470 Transportation Research Board of the National Academies, Washington, D.C., pp.
471 33-39.

472

473 [6] Pérez-Jiménez, F., Barral, M., Soto, J.A. & Navarro, J.A. (2008). Effect of the
474 Nature and Filler Content on Cohesion, Adhesiveness and Rheological Behaviour
475 of the Bituminous Mastics. *Eurasphalt&Eurobitume Congress*, Copenhagen, 21-
476 13 May 2008.

477

478 [7] Pérez-Jiménez, F., Miró, R. & Martínez, A. (2008). Effect of Filler Nature and
479 Content on the Behaviour of Bituminous Mastics. *Road Materials and Pavement*
480 *Design*, Vol. 9, pp. 417-431.

481

482 [8] Faheem, A., Hintz, C., Bahia, H. & Al-Qadi, I. (2012). Influence of Filler
483 Fractional Voids on Mastic and Mixture Performance. *Journal of the*
484 *Transportation Research Record*, No. 2294, Transportation Research Board of the
485 National Academies, Washington, D.C., pp. 74-80.

486

487 [9] Delaporte, B., Di Benedetto, H., Chaverot, P. & Gauthier, G. (2008). Effect of
488 Ultrafine Particles on Linear Viscoelastic Properties of Mastics and Asphalt
489 Concretes. *Journal of the Transportation Research Record*, No 2051,
490 Transportation Research Board of the National Academies, Washington, D.C., pp.
491 41-48.

492

493 [10] Delaporte, B., Di Benedetto, H., Chaverot, P. & Gauthier, G. (2009). Linear
494 Viscoelastic Properties of Bituminous Materials Including New Products Made
495 with Ultrafine Particles. *Road Materials and Pavement Design*, Vol. 10, No. 1,
496 pp. 7-38.

497

498 [11] Clopotel, C., Velasquez, R. & Bahia, H. (2012). Measuring Physico-chemical
499 Interaction in Mastics using Glass Transition. *Road Materials and Pavement*
500 *Design*, Vol. 13, No. S1, pp. 304-320.

501

502 [12] Hesami, E., Jelagin, D., Kringos, N. & Birgisson, B. (2012). An Empirical
503 Framework for Determining Asphalt Mastic Viscosity as a function of Mineral
504 Filler Concentration. *Construction and Building Materials*, Vol. 35, pp. 23-29.

505

506 [13] Hesami, E., Birgisson, B. & Kringos, N. (2014). A new protocol for measuring
507 bituminous mastic viscosity as a function of its filler concentration. *Road*
508 *Materials and Pavement Design*, Vol. 15, No. 2, pp. 420-433.

509

510 [14] Ridgen, P. (1947). The use of Fillers in Bituminous Road Surfacing – A study of
511 filler-binder system in relation to filler characteristics. *Journal of Society of*
512 *Chemical Industry*, No. 66, pp. 9-299.

513

514 [15] Ruiz, C. (1947). Sobre las Propiedades Mecánicas del Sistema Fíller-betún.
515 *Proceedings Segunda Reunión Anual del Asfalto*, Buenos Aires, Argentina,
516 November 17-22, pp. 25-52 (in Spanish).

517

518 [16] Ruiz, C. (1960). *Concentración Crítica de Filler, su Origen y Significado en la*
519 *Dosificación de Mezclas Abiertas*. Dirección de Vialidad de la Provincia de
520 Buenos Aires, Argentina, Publicación N°11.

521

522 [17] Buttlar, W.G., Bozkurt, D., Al-Khateeb, G.G. & Waldhoff, A.S. (1999).
523 Understanding Asphalt Mastic Behavior through Micromechanics. *Journal of the*
524 *Transportation Research Record*, No. 1681, pp. 157-169.

525

- 526 [18] National Cooperative Highway Research Program NCHRP Report XXX for
527 Project 9-45. Test Methods and Specification Criteria for Mineral Filler used in
528 HMA Revised Draft Final Report 12/28/2010 from University of Wisconsin-
529 Madison.
530
- 531 [19] Faheem, A., & Bahia, H. (2011). Modelling of asphalt mastic in terms of filler-
532 bitumen interaction. *Road Materials and Pavement Design*, Vol. 11, Sup 1, pp.
533 281-303.
534
- 535 [20] Shen, S., Airey, G., & Carpenter, S. (2006) A Dissipated Energy Approach to
536 Fatigue Evaluation. *Road Materials and Pavement Design*, Vol. 7, No. 1, pp. 47-
537 69.
538
- 539 [21] Yin, H., Buttlar, W., Paulino, G., & Di Benedetto, H. (2008) Assessment of
540 Existing Micro-mechanical Models for Asphalt Mastics Considering Viscoelastic
541 Effects. *Road Materials and Pavement Design*, Vol. 9, No. 1, pp. 31-57.
542
- 543 [22] Botella, R., Pérez Jiménez, F. & Miró, R. (2012). Application of a Strain Sweep
544 Test to Assess Fatigue Behavior of Asphalt Binders. *Construction and Building*
545 *Materials*, Vol. 36, pp.906-912.
546
- 547 [23] Ahmadinia, E., Zargar, M., Karim, M.R., Abdelaziz, M. & Shafigh, P. (2012)
548 Using waste plastic bottles as additive for stone mastic asphalt. *Materials and*
549 *Design*, Vol. 32, pp. 4844–4849.
550
- 551 [24] IRAM Standard No. 1542 (1983). Material de relleno “filler” para mezclas
552 asfálticas. Método de determinación de la relación crítica (concentración crítica) y
553 de la densidad. Instituto Argentino de Normalización y Certificación, Argentina.
554
- 555 [25] Bressi, S., Dumont, A. & Partl, M (2016). An Advanced methodology for the mix
556 design optimization of hot mix asphalt. *Materials and Design*, Vol. 98, pp. 174-
557 185.
558
- 559 [26] Antunes, P., Ramalho, A. & Carrillo, E. (2014) Mechanical and wear behaviours
560 of nano and microfilled polymeric composite: effect of filler fraction and size.
561 *Materials and Design*, Vol. 61, pp. 50–60.
562
- 563 [27] Antunes, V., Freire, A., Quaresma, L. & Micaelo, R. (2015) Influence of the
564 geometrical and physical properties of filler in the filler–bitumen interaction.
565 *Construction and Building Materials*, Vol. 76, pp. 322-329.
566
- 567 [28] Antunes, V., Freire, A., Quaresma, L. & Micaelo, R. (2016) Effect of the
568 chemical composition of fillers in the filler-bitumen interaction. *Construction and*
569 *Building Materials*, Vol. 104, pp. 85-91.
570
- 571 [29] Movilla-Quesada, D., Raposeiras, A., Castro-Fresno, D. & Peña-Mansilla, D.
572 (2015). Experimental study on stiffness development of asphalt mixtures
573 containing cement and Ca(OH)₂ as contribution filler. *Materials and Design*, Vol.
574 75, pp. 157-163.
575

- 576 [30] Mo, L., Huurman, M., Wu, S., & Molenaar, A. (2009). Ravelling investigation of
577 porous asphalt concrete based on fatigue characteristics of bitumen–stone
578 adhesion and mortar. *Materials and Design*, Vol. 30, pp. 170–179.
579
- 580 [31] Miró, R., Martínez, A. H., Moreno-Navarro, F., & del Carmen Rubio-Gámez, M.
581 (2015). Effect of ageing and temperature on the fatigue behaviour of bitumens.
582 *Materials & Design*, 86, 129-137.
583
- 584 [32] Ward, R. E., & McDougal, J. M. (1979). *Bituminous concrete plant dust*
585 *collection system--effects of using recovered dust in paving mix* (No. FHWA/WV-
586 79-003 Final Rpt.).
587
- 588 [33] Kandhal, P. S., & Parker, F. (1998). *Aggregate tests related to asphalt concrete*
589 *performance in pavements* (No. 405). Transportation Research Board.
590